COMPARISON OF SAR IMAGE DESPECKLING FILTER PERFORMANCE FOR DIFFERENT

Christian Pan Wan Ting[1], Terrence Lin Junyong[2], Ng Zi Yang[3], Felicia Tai[4], Alastair Wee[4]
[1]Raffles Girls' School, 2 Braddell Rise, Singapore 318871
[2]Raffles Institution, One Raffles Institution Lane, Singapore 575954
[3]Temasek Junior College, 2 Tampines Ave 9, Singapore 529564
[4]DSO National Laboratories, 12 Science Park Drive, Singapore 118225

1 Introduction

Synthetic Aperture Radar (SAR) is a remote sensing technique capable of imaging large regions, it is useful for many applications involving the detection of objects seen in military surveillance or environmental monitoring [1]. Speckle is a type of granular noise that greatly deteriorates the quality of images produced by SAR, hence limiting its applications. This inherent phenomenon arises from interference between many scattering echos within a resolution cell [2]. Though the exact patterns may be random, the properties of the surface or target being imaged affect the characteristics of the speckle. Therefore, there are different optimal filters for different types of surfaces.

While there is theoretical research on classifying types of materials or environments and how they reflect signals [3], real SAR environments are too complex to model, and it is difficult to pinpoint exactly how surface features affect the resulting speckle pattern. Filtering simpler images with larger homogeneous regions generally tends to perform better than filtering complex images with edges and intricate textures. With this objective in mind, our goal is to empirically assess and identify optimal despeckling methods for various surface types. By comparing and analysing the performance of common despeckling techniques across a range of surfaces, we aim to determine the most effective filters for enhancing the interpretability of SAR data.

2 Methodology

SAR can be used to map many different kinds of landscapes, like forests, mountains, cities, water etc. We hypothesised that landscapes with different surface properties would not be despeckled to the same extent by the same filters. Where one filter might suppress speckle noise and smooth the image better, another filter might preserve fine textures and details to a higher degree. For these experiments, we proposed that terrain can be grouped into three main types for faster analysis: urban, maritime and rural, as shown in Table 1.

	Urban	**Maritime**	**Rural**
Scatterers	Buildings, ground (concrete, grass)	Water, ships	Vegetation, ground (clay, soil, snow etc.)
Aim of filter	Preserving fine details of	Preserving isolated point	Preserving topological

	closely-packed structures	targets (ships) on a highly homogenous surface	information about the surface

Table 1. Proposed categories of terrain and their differing characteristics

2.1 Dataset

The dataset used is a Sentinel 1 SAR Strip Map Multi-Look image in horizontal transmission and reception (HH) polarisation in ground range detected (GRD) format. 3 patches of size 5000×5000 pixels that correspond with the 3 categories of terrain above were identified. Then, each big patch is further divided into 100 small patches of size 500×500 pixels. To simulate clean-noisy image pairs, the patches were treated as clean images, and a seeded noise pattern following a Gamma distribution was multiplied pixel-wise to each individual small patch to form a noisy image equivalent. The gamma distribution was chosen because it was identified [4, 5, 6] that the foreseen power of a SAR image is gamma-distributed [7, 8, 9]. Meanwhile, real images refer to the unprocessed patches cropped from the dataset.

Simulated images were necessary in order to apply metrics which all require a clean "ground truth" image for the filtered resultant image to be compared to. Applying more metrics that all measure different aspects of a filter's performance created more avenues for quantitative analysis, allowing us to better predict the performance of the filter when applied to random, real speckled SAR images. However, synthetic tests do not fully account for the complexities present in actual SAR data. Therefore, filter application using actual SAR data is necessary to validate the robustness of the filtering approaches to real, random speckle patterns. Our project methodology is summarised in Figure 1.

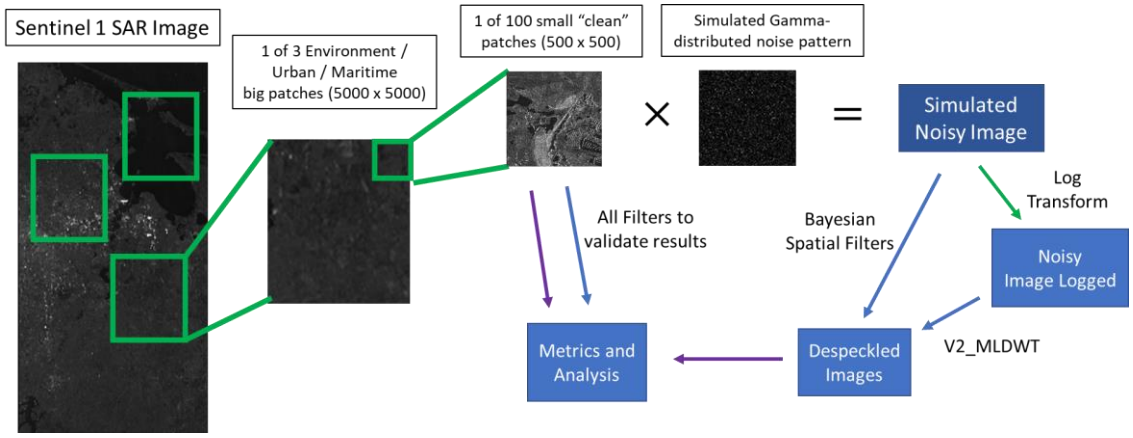

Figure 1. Project Methodology

2.2 Filters

Figure 2 is a diagram showing the categorisation of the filters [9].

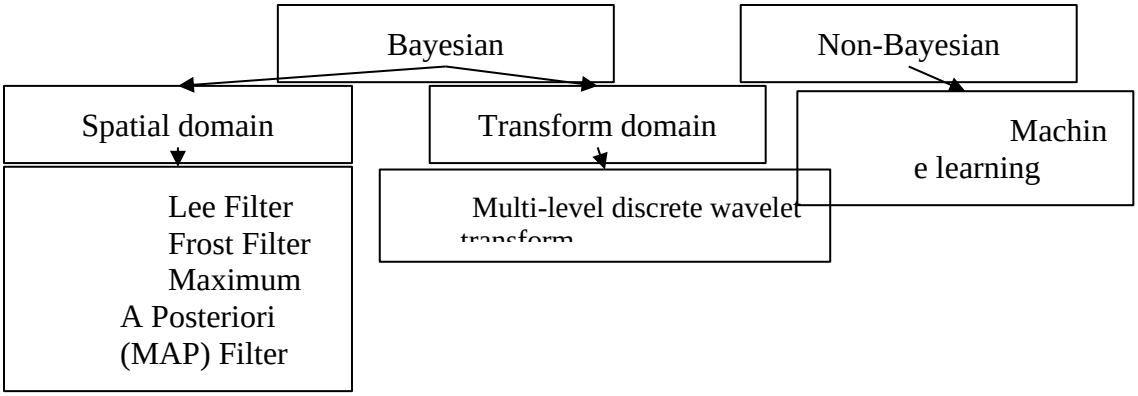

Figure 2. Despeckling Methods

2.2.1 Bayesian Spatial Filters

Bayesian filters in the spatial domain make use of a moving window that calculates the intensity value of the centre pixel using local statistics. The Lee filter uses a standard deviation based filter [10], calculated using Eqn. 1.

$$Intensity = w_m + [1 - \frac{w_v^2 * I_m^2}{w_m^2 * I_v^2}](w_c - w_m) \quad \textbf{(1)}$$

where w_m, w_v *and* w_c are the mean, variance and centre intensity of the window, and I_m and I_v are the mean and variance of the image.

The Frost filter exponentially decreases the weight of the surrounding pixels based on the Euclidean distance (resulting in a circularly symmetric window) before coming up with a weighted average of the window [11] as shown in Eqn. 2. .

$$Intensity = \frac{\sum_{i=1}^{n} I_i * e_i^{-AT}}{\sum_{i=1}^{n} e_i^{-AT}} \quad \textbf{(2)}$$

where I_n is the intensity of pixels in a window, e_i^{-AT} represents weights, A is the damping factor, and T is the Euclidean distance between pixels.

Meanwhile, the Maximum A Posterior (MAP) [12] filter models speckle noise as a gamma distribution as shown in Eqn. 3.

$$Intensity = \frac{(\alpha - L - 1) * I_m + \sqrt{I_m^2 * (\alpha - L - 1)^2 + 4\alpha L I_c I_m}}{2\alpha} \quad \textbf{(3)}$$

where $\alpha = (1 + \frac{1}{L})/(\frac{Variance\ of\ pixel\ values}{I_m^2} - \frac{1}{L})$, L = ENL (in Table 2), and I_m and I_c are the intensities of the window and centre pixel respectively.

When implementing the filters in Python, some parameters are required for the Lee and Frost filters. For the purpose of this comparison, the parameters have been set to: window size (5×5), noise model (multiplicative, Gamma distribution), noise mean (0), noise variance (0.2), and DampFactor (3).

2.2.2 Bayesian Transform Filters

Bayesian filters in the transform domain represent signals as coefficient distributions in the frequency and amplitude domain. Discrete wavelet transform (DWT) decomposes the image into wavelets, and has the advantage of being localised and capable of multi-resolutional analysis unlike Fourier Transforms, improving its performance and adaptability in image denoising. Coefficients are thresholded to filter out details from noise and a cleaner image then reconstructed. Methods of determining an ideal threshold differ by their approach, with some like the Universal Threshold (UT) [13] filtering by amplitudes while others like the Elliptical Wavelet Coefficient Shrinkage (EWCS) [14] utilise distribution instead.

2.2.3 Non-Bayesian Filters

The main non-Bayesian filter chosen was despeckling through machine learning (ML). The model used is the SAR-CNN model [15], trained on 500×500 patches cropped from a separate Sentinel 1-A Strip Map Multi-Look image in HH polarisation in GRD format. For each surface type, 100 patches with added gamma-distributed noise were used, making a total of 300 images. As a state-of-the-art despeckling method, machine learning represents a promising direction for despeckling as it is able to learn an implicit model of the data, allowing it to despeckle data of the same type after training.

Reference	Performance metrics	Mathematical Formula
Does not require a clean image	*Equivalent Number of Looks (ENL)*	$ENL = (\frac{\mu}{\sigma})^2$ where μ is the mean and σ is the standard deviation of the image
Requires a clean image for comparison	*Mean square error (MSE)*	$MSE = E(\hat{f} - f) = \frac{\sum_{i=1}^{n} \hat{f}_i - f_i}{n}$ where $\hat{f}$, f are the intensities of the filtered and speckle-free image respectively and n is the image size
	Structure Similarity Index Metric (SSIM)	$\frac{(2\mu_a\mu_b + P_1)(2\sigma_{ab} + P_2)}{(\mu_a^2 + \mu_b^2 + P_1)(\sigma_a^2 + \sigma_b^2 + P_2)}$ where μ_a, μ_b, σ_a, σ_b and σ_{ab} are the local means, standard deviation and cross variance for the clean and noisy images, a and b. P_1=(0.01*L) and P_2=(0.03*L), where L is the dynamic range of the pixels
	Signal to noise ratio (SNR)	$SNR = 10log_{10}\frac{\sigma}{MSE}$
	Peak signal to noise ratio (PSNR)	$PSNR = 10log_{10}\frac{255 \times 255}{MSE}$

2.2 Filter performance metrics

Table 2. Metrics and formulas

When comparing simulated data, all five metrics listed in Table 2 were used. The utilisation of multiple metrics is crucial as each metric captures different aspects of despeckling performance. While ENL focuses on speckle reduction, SSIM emphasises structural similarity, PSNR and SNR evaluate noise levels, and MSE provides an overall measure of pixel-wise discrepancies For real data, only ENL and visual inspection was used to evaluate the image.

3 Results

3.1 Simulated data

Surface type / Filter		Filter					
		Noisy	**Lee**	**Frost**	**MAP**	**Wavelet**	**Machine Learning**
Urban	PSNR	18.0	**19.8**	19.2	18.7	18.4	19.7
	SNR	0.443	**5.9**	4.93	4.58	4.56	5.79
	MSE	2440	**722**	1390	1570	952	977
	ENL	3.65	5.76	7.99	7.59	**13.1**	6.35
	SSIM	0.628	**0.678**	0.591	0.565	0.417	0.566

Surface type / Filter		Filter					
		Noisy	**Lee**	**Frost**	**MAP**	**Wavelet**	**Machine Learning**
Maritime	PSNR	20.3	24.5	25.3	25.7	25.9	**28.6**
	SNR	-6.60	-1.92	-1.06	-0.655	-0.508	**2.13**
	MSE	680	234	192	176	170	**92.2**
	ENL	2.89	7.52	10.7	14.7	**34.0**	31.8
	SSIM	0.365	0.521	**0.561**	0.519	0.340	0.480

Surface type / Filter		Filter					
		Noisy	Lee	Frost	MAP	Wavelet	Machine Learning
Rural	PSNR	17.8	21.1	21.1	20.8	20.8	**22.3**
	SNR	-3.16	2.05	2.03	1.76	1.69	**3.51**
	MSE	180	503	507	540	549	**391**
	ENL	4.49	9.97	15.6	14.9	**43.9**	15.1
	SSIM	0.487	**0.599**	0.544	0.514	0.301	0.472

Table 3(a), (b) and (c) Quantitative assessment results for urban, maritime and rural image, averaged over 100 distinct images

3.2 Real data

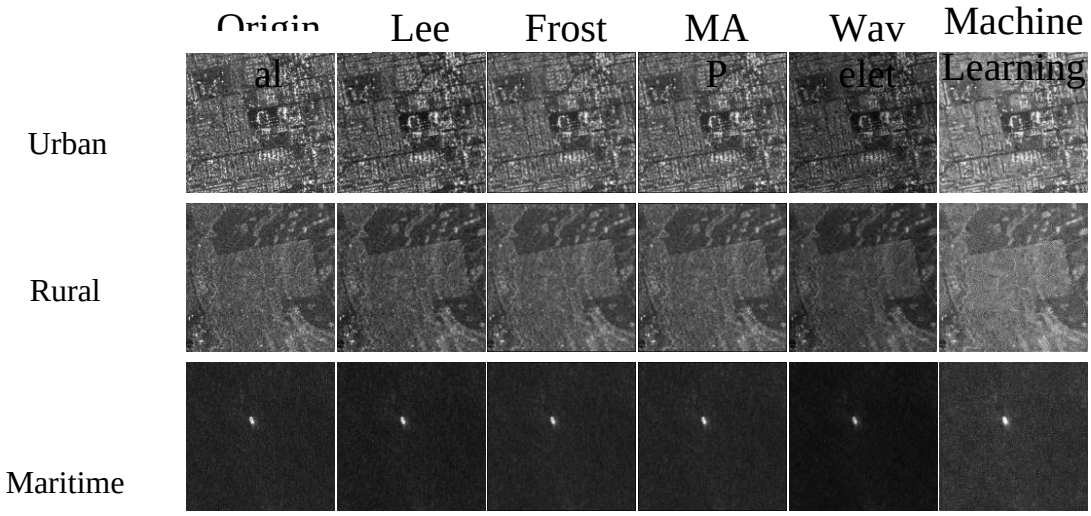

Figure 3. Visual representation of filter performance on real SAR data

Surface type / Filter		Filters				
		Lee	Frost	MAP	Wavelet	Machine Learning
Urban	ENL	4.69	6.17	5.78	**7.32**	6.35

Maritime	ENL	14.2	20.8	18.3	**40.4**	31.8
Rural	ENL	9.79	13.2	12.1	**19.0**	16.6

4 Discussion/Analysis

According to the metrics for simulated noise in Table 3, the Lee filter outperformed all other filters by a significant margin for Urban images. While the Lee filter suppressed speckle, it did so while blurring the image, which was not ideal when the urban environment consisted of densely packed buildings with edges that should be preserved. However, upon visual inspection, it was found that due to the Lee filter's simple formula, it applied the least amount of blurring, allowing it to preserve the most amount of similarity where other filters overcompensated.

For the maritime and rural categories with simulated noise, SAR-CNN had performed relatively well, but did not preserve image similarity (SSIM) as well as its counterparts. Lee on the other hand had poor metrics but preserved image similarity better, possibly due to the greater proportion of homogenous regions like the farmland and water that Lee is better suited for.

The wavelet filter was one of the worst performing, often blurring out the images entirely. This can be attributed to the relatively small size of the images used (500×500 pixels), resulting in fewer coefficients after decomposition. Internal testing showed that the wavelet filter performs significantly better when given input images with larger dimensions. On the contrary, it is actually the best when tested on the real data in terms of ENL. This is because it tends to darken the image, lowering the standard deviation of the pixels in the image and resulting in a lower ENL. This is also the reason why it has the highest ENL in simulated data too.

5 Conclusion

In conclusion, we recommend the Lee filter for urban terrain and the ML filter, trained only on gamma-distributed noise for maritime and rural terrain based on the simulated data. The results from real data are inconclusive because we could only use ENL and the wavelet filter was much better at that metric than the other filters. Not counting the wavelet filter, machine learning also wins for all terrains. It must be noted that our knowledge of the simulated noise gives the ML filter a slight advantage over the rest, which would not exist in a real scenario.

As a further extension to our project, we can hypothesise that different landscapes would not follow the same noise distribution as each other due to differing surface roughness and dielectric constant as it affects how much signal penetrates into the medium, and how much of the energy gets lost to the medium through absorption [2]. Using a SAR dataset that contains both the Multi-Look image and its constituent Single-Look complex images, we can consider the former to be the "clean" image and the latter to be "noisy". Along with this, we can try to find the noise

distribution of the single-look complex images by comparing it with the multi-look images and using an additive and multiplicative noise model like so:

$Noisy = Clean * MNoise + ANoise$ where MNoise and ANoise are the multiplicative and additive noise respectively and ANoise is roughly constant

Acknowledgements

We are profoundly grateful to our research mentors, Felicia and Alastair, for their unwavering guidance and support throughout this journey. Their expertise, encouragement, and invaluable insights have been instrumental in shaping our research experience.

References

1. Arsenios Tsokas, Maciej Rysz, Panos M. Pardalos, Kathleen Dipple, SAR data applications in earth observation: An overview, Expert Systems with Applications, Volume 205, 2022, 117342, ISSN 0957-4174,https://doi.org/10.1016/j.eswa.2022.117342.

2. Meyer, Franz. "Spaceborne Synthetic Aperture Radar – Principles, Data Access, and Basic Processing Techniques." SAR Handbook: Comprehensive Methodologies for Forest Monitoring and Biomass Estimation. Eds. Flores, A., Herndon, K., Thapa, R., Cherrington, E. NASA. 2019. DOI: 10.25966/ez4f-mg98

3. Earth Science Data Systems, N. (2020, April 10). What is Synthetic Aperture Radar? https://www.earthdata.nasa.gov/learn/backgrounders/what-is-sar

4. Oliver C, Quegan S (1998) Understanding synthetic aperture radar images. Artech House, Boston

5. Ulaby FT, Moore RK, Fung AK (1986) Microwave remote sensing, Active and Passive, Volume III. from Theory to Applications, Artech Hous

6. Walessa M, Datcu M (2000) Model-based despeckling and information extraction from SAR Images. IEEE Trans Geosci Remote Sens 38(5):2258–2269

7. Escamilla HM, Méndez ER (1991) Speckle statistics from gamma-distributed random-phase screens. J Opt Soc Am A 8:1929–1935

8. Sathit Intajag and Sakreya Chitwong, (2006) Speckle Noise Estimation with Generalized Gamma Distribution. SICEICASE International Joint Conference, Oct 2006, 18–21, in Bexco, Busan, Korea

9. Singh, P., Diwakar, M., Shankar, A., Shree, R., & Kumar, M. (2021). A Review on SAR Image and its Despeckling. Archives of Computational Methods in Engineering, 28, 4633 - 4653. https://doi.org/10.1007/s11831-021-09548-z

10. Lee, J.-S., 1980, Digital image enhancement and noise filtering by use of local statistics: IEEE Transactions on Pattern Analysis & Machine Intelligence, no. 2, p. 165-168

11. Frost, V. S., Stiles, J. A., Shanmugan, K. S., and Holtzman, J. C., 1982, A model for radar images and its application to adaptive digital filtering of multiplicative noise: IEEE Transactions on Pattern Analysis & Machine Intelligence, no. 2, p. 157-166

12. A. Lopes, E. Nezry, R. Touzi and H. Laur, "Maximum A Posteriori Speckle Filtering And First Order Texture Models In Sar Images," 10th Annual International Symposium on Geoscience and Remote Sensing, College Park, MD, USA, 1990, pp. 2409-2412, doi: 10.1109/IGARSS.1990.689026.

13. D. L. Donoho and I. M. Johnstone, "Adapting to Unknown Smoothness via Wavelet Shrinkage" , Tech. Report # 425, Statistics Dept., Stanford Univ., 1993

14. Langis Gagnon, Alexandre Jouan, "Speckle filtering of SAR images: a comparative study between complex-wavelet-based and standard filters," Proc. SPIE 3169, Wavelet Applications in Signal and Image Processing V, (30 October 1997); doi: 10.1117/12.279681

15. G. Chierchia, D. Cozzolino, G. Poggi and L. Verdoliva, "SAR image despeckling through convolutional neural networks," 2017 IEEE International Geoscience and Remote Sensing Symposium (IGARSS), Fort Worth, TX, USA, 2017, pp. 5438-5441, doi: 10.1109/IGARSS.2017.8128234.